Journal of Environmental Chemical Engineering 12 (2024) 111723

Contents lists available at ScienceDirect

Journal of Environmental Chemical Engineering

journal homepage: www.elsevier.com/locate/jece

Green vs fossil-based energy vectors: A comparative techno-economic analysis of green ammonia and LNG value chains

Federica Restelli *, Marta Gambardella, Laura Annamaria Pellegrini

GASP - Group on Advanced Separation Processes & GAS Processing, Dipartimento di Chimica, Materiali e Ingegneria Chimica "G. Natta", Politecnico di Milano, Piazza Leonardo da Vinci 32, 20133 Milano, Italy

ARTICLE INFO

Editor: Javier Marugan

Keywords:
Green ammonia
Liquefied natural gas
Energy vector
Techno-economic analysis
Social cost of carbon
Levelized cost of energy

ABSTRACT

This study conducts a comparative techno-economic assessment on the value chains of ammonia, as a green energy vector, and Liquefied Natural Gas (LNG), representing the benchmark energy vector, for long-distance energy transportation from Middle East to Europe. The value chain involves production from resources, conversion to an energy vector, storage and transport and reconversion of the energy vector to a suitable fuel. For comparison purposes, an electric power output of 400 MW is assumed to be produced by a power plant that utilizes either green or fossil fuels delivered to it. The adopted parameter for this comparison is the Levelized Cost of Energy (*LCoE*). Greenhouse gas emissions are economically penalized through the Social Cost of Carbon (SCC). Considering a SCC of 0.100 €/kg, the *LCoE* of the LNG value chain is 59.19 €/MWh, while that of ammonia is 231.71 €/MWh. Since the cost of producing green hydrogen and purified natural gas strongly affects the results, a sensitivity analysis is performed to assess the impact of the assumed values. The SCC required to break even the *LCoE* of the two value chains is: 0.183 €/MWh when considering the most favorable scenario for the green energy vector (low green hydrogen and high purified natural gas production costs) and 1.731 €/kg when considering the most unfavorable one. This study highlights the cost-effectiveness of LNG in the current economic and regulatory landscape. However, the break-even range for the SCC indicates the potential for green ammonia to gain economic viability under higher carbon pricing scenarios.

1. Introduction

The exploitation of renewable energy sources (RES) is playing a key role in tackling the issues related to climate change and energy security. There is a general consensus that energy storage is crucial in order to overcome the inherent variability of RES and enhance their contribution to overall power generation. Consequently, future energy systems necessitate effective and affordable techniques for storing energy. To date, various mechanical, electrical, thermal, and chemical methods have been devised to store electrical energy for large-scale utility services. Storage solutions such as batteries or redox cells are unlikely to have the required capacity for large-scale energy storage. Pumped hydro and techniques like compressed gas energy storage encounter limitations due to geological factors that restrict their implementation. The sole flexible mechanism capable of storing vast amounts of energy over extended periods, regardless of location, is chemical energy storage. The storage of energy in chemical form can be accomplished through hydrogen (H_2), called "green H_2" when it is produced through RES-driven water electrolysis, or carbon-neutral hydrogen derivatives, such as ammonia (NH_3), called "green ammonia" when it is synthesized from green hydrogen. NH_3 is considered a promising energy vector, given its chemical and physical properties, which are summarized in Table 1. Moreover, the infrastructure for transporting and storing ammonia is already established, given its role as the world's second-largest chemical commodity. Ammonia serves multiple purposes, including being employed as an agricultural fertilizer, a feedstock for food production, an industrial material, a refrigerant, and an additive.

NH_3 is gaseous under atmospheric conditions of temperature and pressure. Ammonia liquefaction is usually performed in order to reduce the storage volume and requires compression to 8.6 bar at room temperature or cooling to − 33.4 °C at atmospheric pressure. Cryogenic storage at atmospheric pressure is seen as the most cost-effective option for large capacities. These liquefaction conditions are mild, especially when compared to methane (CH_4), which has a molecular weight similar to that of ammonia, and liquefies at − 166 °C and atmospheric pressure. The higher boiling point of ammonia is due to the strong intermolecular hydrogen bonds. Thus, shipping ammonia has low investment and

* Corresponding author.
E-mail address: federica.restelli@polimi.it (F. Restelli).

https://doi.org/10.1016/j.jece.2023.111723
Received 26 August 2023; Received in revised form 7 November 2023; Accepted 12 December 2023
Available online 14 December 2023

Nomenclature

A_j	Characteristic size of equipment j.
$B_{i,j}$	Constants for calculating the bare module factor of equipment j ($i = 1,2$).
C	Purchased cost.
$CAPEX_t$	Capital expenditures at the year t.
$C_{BM,j}$	Bare module cost of equipment j.
$C^0_{BM,j}$	Bare module cost of equipment j constructed with carbon steel and operating under atmospheric pressure.
$C^0_{p,j}$	Purchased base cost of equipment j.
C_{fuel}	Cost of fuel.
C_{OL}	Cost of operating labor.
$Cons_{\text{fuel}}$	Fuel consumption rate.
$Crew$	Number of people in a ship's crew.
C_{RM}	Cost of raw material.
$C_{TM,j}$	Total module cost of equipment j.
C_{UT}	Cost of utilities.
C_{WT}	Cost of waste treatment.
DMC	Direct Manufacturing Costs.
e_{fuel}	CO_2 emissions per volume of fuel.
E_{fuel}	CO_2 emissions rate of fuel.
F	Energy vector production rate.
$F_{BM,j}$	Bare module factor of equipment j.
FMC	Fixed Manufacturing Costs.
$F_{M,j}$	Material factor of equipment j.
$F_{P,j}$	Pressure factor cost of equipment j.
F_{TOT}	Total molar flow rate.
GE	General Expenses.
H_{eq}	Plant availability.
I	Cost Index.
$K_{i,j}$	Constants for calculating the purchase equipment cost of equipment j ($i = 1,2,3$).
$LCoE$	Levelized Cost of Energy.
LHV	Lower Heating Value.
$OPEX_{\text{CO2}}$	Operating expenditures associated with the CO_2 emissions.
$OPEX_{\text{fuel}}$	Operating expenditures associated with the fuel consumption.
$OPEX_{\text{labor}}$	Operating expenditures associated with the operating labor.
$OPEX_t$	Operating expenditures at the year t.
T	Temperature.
T_{IN}	Inlet temperature.
T_{NBP}	Normal boiling point temperature.
T_{OUT}	Outlet temperature.
P	Pressure.
P_{IN}	Inlet pressure.
P_{OUT}	Outlet pressure.
r	Discount rate.
ρ	Volumetric density.
SCC	Social Cost of Carbon.
t	Year index.
$t_{\text{loading and unloading}}$	Time for loading and unloading operations.
$t_{\text{return trip}}$	Time for the return trip.
$t_{\text{safety buffer}}$	Time to account for potential delays.
t_{storage}	Time in which the energy vector must be stored.
V_{storage}	Storage tank volume.
V_{vessel}	Vessel volume.

operating costs due to the ease of the liquefaction operation and liquid storage. This feature is of interest for the use of ammonia as a green hydrogen carrier since it avoids criticalities and high costs related to pure hydrogen transportation. Indeed, since hydrogen, as methane, liquefies at cryogenic temperatures, its liquefaction is an energy-intensive process and its storage and shipping require high-quality insulation material. Moreover, when hydrogen content is considered, liquid ammonia has the highest volumetric hydrogen density at atmospheric pressure (121 kg_{H2}/m^3, calculated as the product between its gravimetric hydrogen fraction and its volumetric density) among commonly considered hydrogen carriers [3–7], as shown in Fig. 1. Liquefied ammonia (LNH_3) volumetric hydrogen density is 1.5 times higher than that of liquefied hydrogen (LH_2) because ammonia is ten times denser than LH_2. In addition, it is more than twice higher as that of liquid organic hydrogen carriers (LOHC).

The ammonia volumetric energy density is lower, but comparable, than that of carbon-based fuels, and it is higher than that of liquefied hydrogen, as reported in Fig. 2.

This property suggests the possibility of using ammonia as fuel. However, burning pure ammonia is challenging due to its combustion properties. A comparison with CH_4 is reported in Table 2. Ammonia presents low laminar burning velocity, narrow flammability limits and high minimum ignition energy. Thus, combustion needs a high amount of energy to start and then the flame propagates slowly releasing less heat than methane flame, as revealed by the difference in the adiabatic temperature.

Direct use of ammonia in Solid Oxide Fuel Cells (SOFC) is studied by research groups for small-scale energy production with an efficiency of 40–60% [2]. A temperature above 700 °C is required to generate high electrical power by the supply of pure ammonia, without any additional operation but preheating. Among the ongoing projects, Kyoto University is developing a 1 kW SOFC with a nickel-based catalyst, which is the most powerful device known [10].

NH_3 in Internal Combustion engines (ICE) has already been applied for buses during the Second World War in Belgium, due to the shortage of fossil fuels. Even if this solution was abandoned as soon as the fossil

Table 1
Properties of ammonia [1,2].

Property	Value
Molecular weight [kg/kmol]	17.031
Normal boiling point (T_{NBP}) [°C]	-33.4
Liquid density at T_{NBP} [kg/m^3]	682.6
Vapor pressure at 20 °C [bar]	8.58
Gravimetric hydrogen density [kg_{H2}/kg_{NH3}]	0.18
Heat of vaporization at T_{NBP} [MJ/kg]	1.371
Lower Heating Value (LHV) [MJ/kg]	18.6

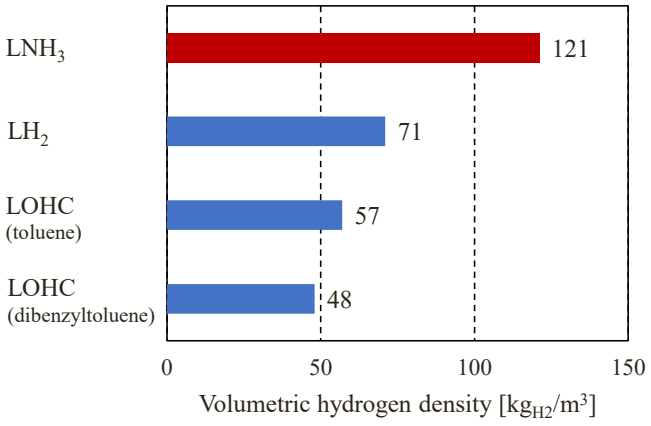

Fig. 1. Comparison of hydrogen carriers' volumetric hydrogen density [kg/m^3].

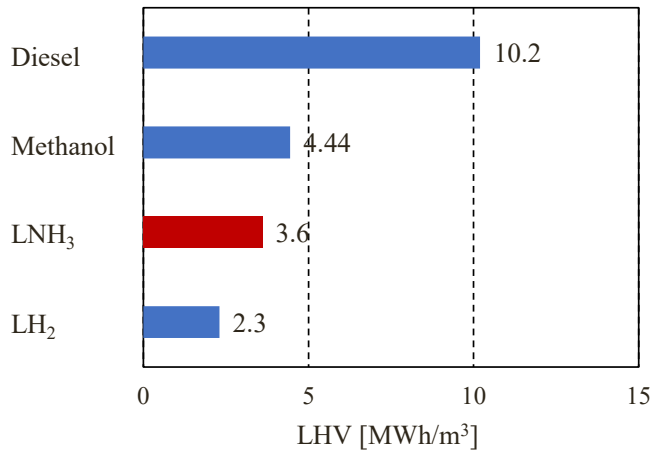

Fig. 2. Comparison of fuel LHV on a volume basis [MWh/m^3].

fuel shortage ended, it showed the potential of ammonia as fuel. Currently, ammonia-fueled ICE are of interest, especially in the marine sector. Several naval companies are developing ammonia-powered motors: for instance, MAN energy solution declares the commercialization of a two-stroke engine by 2024. A Norwegian consortium led by Wärtsilä is developing a four-stroke ammonia engine [11]. Mitsui O.S.K Lines is constructing a large-scale ammonia carrier powered by ammonia itself [12]. Japanese companies are investing in the development of pure ammonia gas turbines [13]. This technology is advantageous because, as for the SOFC, preheating is the only process needed once ammonia is transported to the end users. On the other hand, the need to design and construct new models of gas turbine increases the investment costs and the commissioning times. Mitsubishi Power has announced the commercialization of a 40 MW technology by the year 2025 [14]. The IHI Corporation aims to commercialize a 2 MW gas turbine by the end of 2023 [15]. The SIP energy carrier program is developing a 100 MW gas turbine, commercially available by 2030 [8].

Researchers are developing methods to enhance ammonia combustion properties and to design suitable burners. The improvement of the combustion characteristics is usually achieved by blending ammonia with other fuels. A bench-scale 1.2 MW coal-fired furnace was investigated for ammonia co-firing [16]. The experimental study reveals that ammonia co-firing is feasible with modifications to the coal combustion system and leads to a decrease in the carbon dioxide emissions. Therefore, retrofitting existing coal-fired plants is a possible and advantageous solution. Furthermore, the same study analyzes pure ammonia firing by progressively diminishing the coal supply. It results in less power generated than the co-firing solution, but the combustion proceeds stably, and NO_x emissions were not an issue with proper air-staging [16].

In addition to blending ammonia with fossil fuels, the possibility of blending it with hydrogen is being studied. In particular, the partial cracking of ammonia is considered advantageous because it improves the properties of ammonia without requiring as much energy as is needed for the total decomposition. Moreover, as demonstrated experimentally [9], 28% cracked ammonia burns in hydrocarbon-fired gas-turbine burners, attaining performances comparable to those of fossil fuels, as reported in Table 2. The possibility of exploiting a technology already present in the market reduces the capital investment and the time for commercialization. A concern with ammonia combustion is the NO_x emissions due to the nitrogen atoms in the molecule. Nonetheless, technologies for abatement of NO_x emissions, such as selective catalytic reduction [17], are well-established and commercially available. Another environmental concern is related to the possible ammonia leakages, which cause soil acidification and promote the formation of particulate matter [18]. However, ammonia is a global commodity, hence, regulations and standards, along with training protocols, have already been established to ensure safe handling and transport [11].

For the presented reasons, the International Energy Agency (IEA) discusses ammonia as a future electricity-based fuel in its report [18]. Similarly, the International Renewable Energy Agency (IRENA) defines ammonia as one of the energy carriers of the 21st century [11] and the International Maritime Organization (IMO) identifies ammonia as the green fuel to halve greenhouse gas emissions of the shipping sector by 2050 [13]. Furthermore, Japan's Natural Resources and Energy Agency presented a roadmap to be carbon neutral by 2050, in which the deployment of ammonia for energy production plays a key role [19]. However, the use of ammonia as a fuel still needs to be approved by the relevant authorities. Currently, neither the IMO nor the fuel regulatory authorities endorse this ammonia application [11].

Few techno-economic evaluations on the value chain of ammonia as an energy vector are present in the literature. The work by Song et al. [20] explores the potential of using offshore wind energy in China to produce hydrogen and supply it to Japan using three potential transport mechanisms: LH_2, methylcyclohexane (MCH) as a LOHC, and LNH_3. The authors consider separately the costs associated with the delivery of ammonia without dehydrogenation at the destination, recognizing that ammonia could be employed directly as a fuel in power generation. Wijayanta et al. [21] compare different storage options for hydrogen, including LH_2, MCH, and LNH_3. The results highlight that ammonia's direct use, as fuel or feedstock, is a promising option for storing and utilizing hydrogen efficiently in different sectors. The work by Giddey et al. [22] analyzes four pathways for the ammonia energy chain, two of which include the ammonia direct use for power generation, either in Solid Oxide Fuel Cells or blended with diesel, kerosene or methanol in Internal Combustion Engines. It concludes that the overall efficiency of the entire ammonia energy chain is higher when it is directly utilized in SOFC or ICE, despite underlying their low technological maturity. The authors emphasize the importance of developing efficient and sustainable ammonia production methods, as well as the integration of ammonia into existing energy systems, to support the transition to a renewable energy future.

Salmon and Bañares-Alcántara [23] perform a review study on the potential of green ammonia as an energy carrier. This work explores the concept of using renewable energy sources to produce ammonia and suggests that it can serve as a versatile and scalable spatial energy vector, enabling the transport and storage of renewable energy across regions. The article emphasizes the role of green ammonia in supporting decarbonization efforts and fostering a sustainable energy system.

The review study conducted by Cardoso et al. [24] addresses the issues related to the utilization of pure ammonia as a fuel, delving into the fundamental mechanisms necessary for developing the combustion of pure ammonia within internal combustion engines. While the primary

Table 2
Combustion properties of methane, ammonia and 28% cracked ammonia[2,8,9].

Fuel	Laminar burning velocity [cm/s]	Flammability limits	Minimum ignition energy [mJ]	Lower heating value [MJ/kg]	Adiabatic flame temperature [°C]
CH_4	37	0.5-1.7	0.28	50	1,950
NH_3	7	0.6-1.4	8	18.6	1,800
28% cracked NH_3	30		0.25		

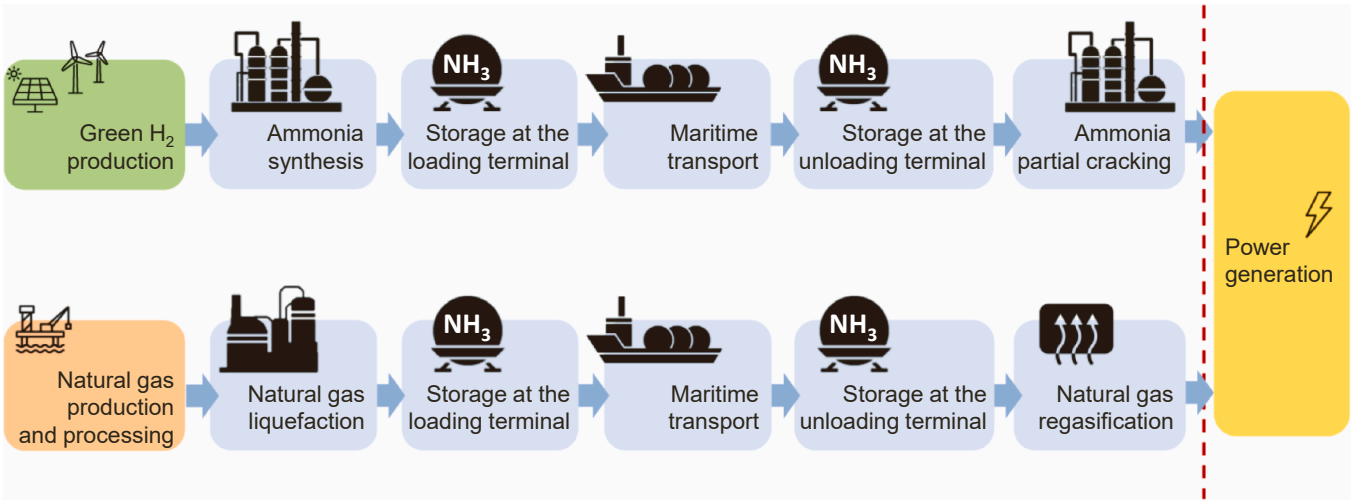

Fig. 3. LNH_3 and LNG value chains.

focus is on the operation of pure ammonia and ammonia fuel blends, the review also extensively explores the issues related to controlling NO_x emissions, the current challenges in understanding ammonia chemistry in detail, as well as the absence of high-fidelity numerical models. These factors are discussed in the context of their contribution to facilitating the widespread adoption of this technology.

Estevez and coauthors' review [25] focuses on the assessment of green ammonia's potential for various energy applications, such as serving as an energy carrier, an electricity generator, and an E-fuel. Furthermore, the study explores recent research that proposes the use of nitrogen-based compounds, like urea, hydrazine, and ammonium nitrate, as alternative fuels. It also examines the feasibility of utilizing other nitrogen-based compounds, thereby providing an updated perspective on the entire ecosystem surrounding green ammonia, from production to consumption, including storage and transportation. Additionally, the review identifies the forthcoming challenges in achieving a technically and economically feasible energy transition.

The review study by Valera-Medina et al. [26] comprehensively explores the role of ammonia as an energy vector. It covers all aspects, from production, distribution, utilization, safety, legal considerations, and economic aspects in supporting future energy needs. The study also delves into the fundamentals of combustion and practical cases for ammonia energy recovery. It outlines the potential of ammonia in mitigating carbon emissions, considering the advantages and limitations of its use for energy storage. The review benefits from the latest insights from experts actively involved in this field, offering insights into the progress in ammonia's use as an energy carrier.

To the authors' knowledge, there is no comparison in the literature between an energy vector produced from RES, such as liquefied ammonia, which is a good candidate given its properties and the results of the cited studies, and a traditional fossil-based energy vector, such as Liquefied Natural Gas (LNG). Both LNH_3 and LNG can be stored in large quantities and transported across long distances, allowing countries that lack proper energy resources to access them from remote locations and diversify their energy supply, enhancing energy security and promoting economic and geopolitical stability. Currently, LNG is adopted to this purpose. However, given the increasing concerns about climate change, other carriers, not originated from fossil resources, have to be investigated to replace LNG.

The present article aims to compare the value chains of LNH_3, as a carbon-free energy vector, and LNG, representing the benchmark energy vector, from a techno-economic point of view. The value chain consists of production from resources, conversion to an energy vector, storage and transport, reconversion of the energy vector to a fuel suitable to be burned in an ICE. For the LNH_3 value chain, the last step is partial cracking with a conversion of 30% in order to obtain a mixture of ammonia, hydrogen and nitrogen (N_2) with combustion properties similar to that of hydrocarbons. A case study of energy delivery from Middle East to Europe via maritime transport is considered. The main processes of the value chains, ammonia synthesis and partial cracking and natural gas liquefaction and regasification, are simulated using the Aspen Plus® V11 [27] commercial software simulator. The derived material and energy balances serve as the basis for assessing the capital and operating expenditures of the process plants. The starting resources are renewable energy and raw natural gas. The cost of producing green H_2 and purified natural gas strongly depends on assumptions such as location (onshore/offshore), type of renewable power plant, type of reservoir. A sensitivity analysis on the production costs of both green H_2 and natural gas is performed to assess the impact of the assumed values on the results. The levelized cost of energy method is used for the economic assessment [28]. The Social Cost of Carbon (SCC) required to break even the levelized cost of energy of the two value chains is calculated. The novelty of this work lies in the establishment of a methodology for quantifying the costs associated with energy vectors used for long-distance energy transport. By accounting for the cost of greenhouse gas emissions, this methodology makes it possible to estimate the cost gap between green and fossil-based energy vectors. If this gap were bridged with appropriate policies, green energy vectors would become cost-competitive, as well as environmentally beneficial, in comparison to their fossil-based counterparts.

2. Modeling, methods and methodology

2.1. Basis of design

In this study, the energy transportation from a theoretical energy production site in the Middle East to a theoretical utilization site in Europe is assumed, spanning a sea distance of 5000 km.

Two value chains are considered: one involving green ammonia as a carbon-free energy vector and the other involving LNG as a traditional fossil-based energy vector.

An electric power output of 400 MW is supposed to be produced by a power plant with an efficiency of 56% [29]. The fuel flow rate is calculated to satisfy this output.

Green hydrogen is supposed to be produced at a pressure of 20 bar (typical conditions at the outlet of alkaline electrolyzers [30]) and a temperature of 25 °C. The value chain of the green energy vector (Fig. 3) includes: green hydrogen production, ammonia synthesis and liquefaction at atmospheric pressure, storage at the loading terminal, sea shipping, storage at the unloading terminal and partial cracking to obtain a

Table 3
Assumptions for the economic evaluation.

Item	Value
Base year	2022
Project lifetime	25 y
Discount rate	5%
Plant availability (H_{eq})	8,000 h/y
Construction period	3 y (*CAPEX* breakdown: 40%, 30%, 30%)
Decommission cost	5% *CAPEX* [34]
Exchange rate (2022)	0.951 €/US-$ [35]

mixture of $NH_3/H_2/N_2$ suitable to be burned in a traditional engine.

Purified natural gas is supposed to be available at 40 bar and 25 °C (typical conditions at the outlet of the acid gas purification section [31, 32]). The value chain of the fossil-based energy vector (Fig. 3) includes: natural gas production and processing, liquefaction at atmospheric pressure, storage at the loading terminal, sea shipping, storage at the unloading terminal and regasification. The product delivered is natural gas to be burned in a power cycle.

In these value chains, the main process plants are the ammonia synthesis and partial cracking and the natural gas liquefaction and regasification. Conducting a comprehensive assessment of their investment and operating expenses is crucial to ensure a reliable economic evaluation.

The system boundaries are from the production of the energy vector to its utilization as fuel in a power generation plant, which is not included inside the boundaries. The amount of energy transported differs between the investigated options because of the inherent different production capacity of hydrogen from RES, which is limited by space constraints, and of natural gas from reservoirs, which is generally high. The production capacity of green hydrogen is assumed to be 650 t/d, as for the large-scale NEOM project [33], while the one of natural gas is supposed to be 4 Mt/y. To give each value chain its costs and to be able to compare them, the cost of each block is multiplied by the fraction of fuel utilized to the total fuel delivered.

2.2. Methodology of techno-economic assessment

The Levelized Cost of Energy (*LCoE*) [28] is used to evaluate the cost of the energy vector for both the entire value chain and individual steps, as outlined in Section 2. Its value is calculated according to Eq. (1):

$$LCoE = \frac{\sum_{t=0}^{N-1} \frac{CAPEX_t + OPEX_t}{(1+r)^t}}{\sum_{t=0}^{N-1} \frac{F_{fuel,out} \cdot LHV_{fuel}}{(1+r)^t}} \quad (1)$$

where t represents the year (with 0 being the base year and N-1 being the last year), $CAPEX_t$ and $OPEX_t$ are respectively the capital and operating expenditures at the year t, r is the discount rate, $F_{fuel,out}$ is the flow rate of fuel delivered yearly and LHV_{fuel} is its lower heating value. The financial assumptions are reported in Table 3.

A Social Cost of Carbon (SCC) of 0.100 €/kg-CO_2 (price of emissions allowances traded on the European Union's Emissions Trading System (ETS), record reached in February 2023 [36]) is assumed in the base case in order to penalize the direct CO_2 emissions. Then, the SCC required to break even the levelized cost of energy of the two value chains is calculated as the production costs of green hydrogen and purified natural gas vary.

2.2.1. Process plants

The Turton methodology [37] is used to evaluate the costs of the main processes, ammonia synthesis and cracking and natural gas liquefaction and regasification. This methodology enables a rough estimation of the plant costs and should be regarded as an initial feasibility study.

The capital expenditures (*CAPEX*) of the plant are determined using the Guthrie method [38]. This method calculates the purchased base cost ($C^0_{p,j}$), for the equipment piece j, as:

$$\log_{10}\left(C^0_{p,j}(2001)\right) = K_{1,j} + K_{2,j}\log_{10}(A_j) + K_{3,j}\left[\log_{10}(A_j)\right]^2 \quad (2)$$

where A_j represents a characteristic size of the equipment and the constants $K_{1,j}$, $K_{2,j}$ and $K_{3,j}$ depend on the type of equipment and are available in the book by Turton et al. [37]. The Eq. (2) allows for the evaluation of equipment cost as of the year 2001. To update this cost to the current timeframe, economic inflation must be considered. This adjustment can be accomplished using the following formula:

$$C_{current} = C_{base}\left(\frac{I_{current}}{I_{base}}\right) \quad (3)$$

where C represents the purchased cost, I a cost index and the subscripts indicate different points in time. In this analysis, the Chemical Engineering Plant Cost Index (*CEPCI*) is used as cost index, with $CEPCI_{2001} = 397$ and $CEPCI_{2022} = 816.5$.

To account for the impact of construction material and the operating pressure on equipment cost, the concept of the bare module cost ($C_{BM,j}$) is introduced, which is computed as follows:

$$C_{BM,j} = C^0_{p,j}F_{BM,j} = C^0_{p,j}\left(B_{1,j} + B_{2,j}F_{M,j}F_{P,j}\right) \quad (4)$$

where the bare module factor ($F_{BM,j}$) is a function of the material factor ($F_{M,j}$), influenced by the choice of construction material, and the pressure factor ($F_{P,j}$), accounting for the operating pressure of the equipment. The constants $B_{1,j}$ and $B_{2,j}$ depend on the type of equipment and are available in [37].

The bare module cost for equipment constructed with carbon steel and operating under atmospheric pressure, $C^0_{BM,j}$, and the bare module factor for equipment in these conditions, $F^0_{BM,j}$, are computed with $F_{M,j} = F_{P,j} = 1$.

Starting from the bare module cost, the total module cost (C_{TM}) is derived using Eq. (5), which factors in a 18% increase for contingency expenses and fees. The *CAPEX* accounts for expenses related to site development, off-sites, auxiliary buildings and utilities (grassroots cost) by increasing the C_{TM} as in Eq. (6).

$$C_{TM} = 1.18\sum_j C_{BM,j} \quad (5)$$

$$CAPEX = C_{TM} + 0.5\sum_j C^0_{BM,j} \quad (6)$$

The operating expenditures (*OPEX*) are the costs related to the daily operation of a process plant, calculated as the sum of different cost items, that fall within three main categories:

- Direct Manufacturing Costs (*DMC*), which vary with the production rate and include the costs of raw materials (C_{RM}), utilities (C_{UT}), operating labor (C_{OL}), waste treatment (C_{WT}), direct supervisory and clerical labor, maintenance and repairs, operating supplies, laboratory charges, patents and royalties;
- Fixed Manufacturing Costs (*FMC*), which are unaffected by the production rate and include local taxes, insurance and plant overhead costs;
- General Expenses (*GE*), which include the costs of administration, distribution and selling, research and development.

Estimating *OPEX* necessitates knowledge or, at the least, estimations of the following costs: *CAPEX*, cost of raw materials, utilities, operating labor and waste treatment. Factors for estimating *DMC*, *FMC* and *GE* are reported in Table 4.

C_{RM} is the cost of chemical feedstocks needed for the process. In the current analysis, it is neglected as green hydrogen and purified natural

Table 4
Factors for estimating OPEX [37].

Cost item	Calculated as
DMC	C_{UT}+ 1.33·C_{OL}+ 0.069·*CAPEX*+ 0.03·*OPEX*
FMC	0.708·C_{OL}+ 0.068·*CAPEX*
GE	0.177·C_{OL}+ 0.009·*CAPEX* + 0.21·*OPEX*
OPEX (DMC+FMC+GE)	C_{UT}+ 2.215·C_{OL}+ 0.24·*OPEX*+ 0.146·*CAPEX*

gas are the sole feedstocks, with their production costs already considered in the first block of the value chain. C_{UT} is the cost related to the consumption of electricity and cooling water (CW). For this analysis, specific utility costs of 50 €/MWh for the electric power and 0.015 €/t for the CW, available at 20 °C, are utilized. Utility consumption is determined through the energy balance obtained by process simulation. C_{OL} is the cost of personnel needed for operating the plant. It depends on the required workforce per shift and on the average annual operator salary, assumed to be 40,000 €. The calculation of the required personnel takes into account that an individual operator works an average of 45 weeks in one year, completing five 8-hour shifts weekly. The cost of waste treatment is not considered in this analysis.

2.2.2. Sea transport

The maritime transport of the liquefied energy vector involves the *CAPEX* associated with the acquisition of the ships and the *OPEX* associated with the labor, fuel and CO_2 emissions costs, maintenance and insurance.

The volume to be shipped is computed on the basis of the time in which the energy vector must be stored ($t_{storage}$) defined as:

$$t_{storage} = t_{return\ trip} + t_{loading\ and\ unloading} + t_{safety\ buffer} \quad (7)$$

where $t_{return\ trip}$ is the time for the return trip, $t_{loading\ and\ unloading}$ is the time needed for loading and unloading operations, assumed equal to one day, and $t_{safety\ buffer}$ is a reasonable time to account for potential delays, assumed to be two days. Given a ship speed of 16 knots (approximately 30 km/h), the required storage time amounts to about 17 days.

Considering that, for safety reasons, a maximum of 98% of the ship's capacity can be utilized and that a certain amount of residue, assumed to be 4% by volume [39], must be retained in the ship's tanks for cooling purposes, the calculation of the gross shipping capacity (V_{vessel}), in m^3, is performed as follows:

$$V_{vessel} = \frac{F \cdot t_{storage}}{\rho_{vector} \cdot (0.98 - 0.04)} \quad (8)$$

where F [kg/d] is the energy vector production rate and ρ_{vector} is its volumetric density, equal to 677 kg/m^3 for liquefied ammonia and 450 kg/m^3 for LNG.

The investment costs associated with the ship are retrieved from literature case studies.

The labor cost ($OPEX_{labor}$), in M€/y, is computed according to Eq. (9). It is assumed that two complete crews, each with a size denoted as *Crew*, alternate over the course of one year and that the individual operator receives an annual salary (C_{labor}) of 52,000 €/y.

$$OPEX_{labor} = C_{labor} \cdot Crew \cdot 2 \cdot 10^{-6} \quad (9)$$

It is assumed that ships are powered by conventional fuel engines such as IFO 380 (Intermediate Fuel Oil with a sulfur content lower than 3.5%). The fuel cost (C_{fuel}) is assumed to be 580 €/t. The crew size and the fuel consumption ($Cons_{fuel}$, in t/d) are obtained from technical data sheets of vessels nearly identical in capacity to the ones considered in this work. Therefore, the operating cost related to fuel consumption ($OPEX_{fuel}$), in M€/y, is computed as follows:

$$OPEX_{fuel} = C_{fuel} \cdot Cons_{fuel} \cdot \frac{t_{returntrip}}{t_{storage}} \cdot \frac{H_{eq}}{24} \cdot 10^{-6} \quad (10)$$

Taking into account a value for the CO_2 emissions per volume of IFO (e_{fuel}) amounting to 11.24 kg_{CO2}/$gallon_{IFO}$ [40], the operating cost related to CO_2 emissions ($OPEX_{CO2}$) in M€/y is computed as:

$$OPEX_{CO_2} = E_{fuel} \cdot SCC \cdot \frac{t_{returntrip}}{t_{storage}} \cdot \frac{H_{eq}}{24} \cdot 10^{-6} \quad (11)$$

where E_{fuel} [t/d] represents the CO_2 emissions rate, computed as:

$$E_{fuel} = \frac{Cons_{fuel} \cdot e_{fuel} \cdot 264.2[gallon/m^3]}{\rho_{IFO}} \quad (12)$$

where ρ_{IFO} represents the volumetric density of IFO, with a value of 990 kg/m^3.

2.2.3. Storage

Storage of the energy vector is required at both the loading and unloading terminals. This involves the *CAPEX* associated with the acquisition of the storage tanks and the *OPEX* related to maintenance and insurance. The energy vector is stored in liquid form under a pressure of 1.3 bar, inside spherical tanks equipped with a suitable insulation to limit the heat transfer from the surroundings. The boil-off losses are neglected given the possibility to recondense the boil-off gas at the loading terminal and to redirect it to the reconversion process at the unloading terminal.

The investment costs associated with the tanks are retrieved from literature. For each terminal, the total capacity to be stored ($V_{storage}$ [m^3] in Eq. (13)) is calculated considering the storage of the shipped volume V_{vessel} with a 10% increment to accommodate potential delays.

$$V_{storage} = (1 + 0.1) \cdot V_{vessel} \quad (13)$$

The operating costs for storage are calculated as 10% of the *CAPEX*.

3. Results and discussion

3.1. Green energy vector

Green ammonia is synthesized from hydrogen, which is obtained by RES-driven water electrolysis. The cost of producing green hydrogen depends on different factors, including the type of renewable power plant (wind/solar/…), location (onshore/offshore), the presence of batteries for electricity storage, or electricity supply from the grid through a Power Purchase Agreement (PPA) contract with a portfolio of RES plants, and the electrolyzer technology (alkaline/proton exchange membrane/solid oxide electrolyzer). A green hydrogen cost of 180 €/MWh is assumed in the base case. This value, equivalent to 6 €/kg, is the one obtained in Ref. [41] for a green hydrogen plant, based on a photovoltaic power plant coupled with alkaline electrolyzers and located in the Center of Italy. The simulation of hydrogen production is not included due to the high dependence of its cost on the assumptions, such as the type of electrolyzer and renewable power plant. To maintain a general approach, a sensitivity analysis on the production costs of green hydrogen is performed. The investigated range is 60 - 400 €/MWh. According to Ref. [41], values in the range 120 - 330 €/MWh are realistic and express the current scenario, while values below 120 €/MWh represent an optimistic reduction in costs due to higher technologies' efficiency and lower cost of materials. Values above 330 €/MWh signify a pessimistic increase in costs, which may be caused by material shortages. The techno-economic assessment of the other blocks of LNH_3 value chain, synthesis and liquefaction, maritime transport, storage and partial cracking, is detailed in the following sections.

3.1.1. LNH_3 – synthesis and liquefaction

The synthesis of NH_3 starting from green hydrogen necessitates a supply of N_2 to the process. Nitrogen is obtained by air separation. Since a potential use of the oxygen produced is not conceived in the process,

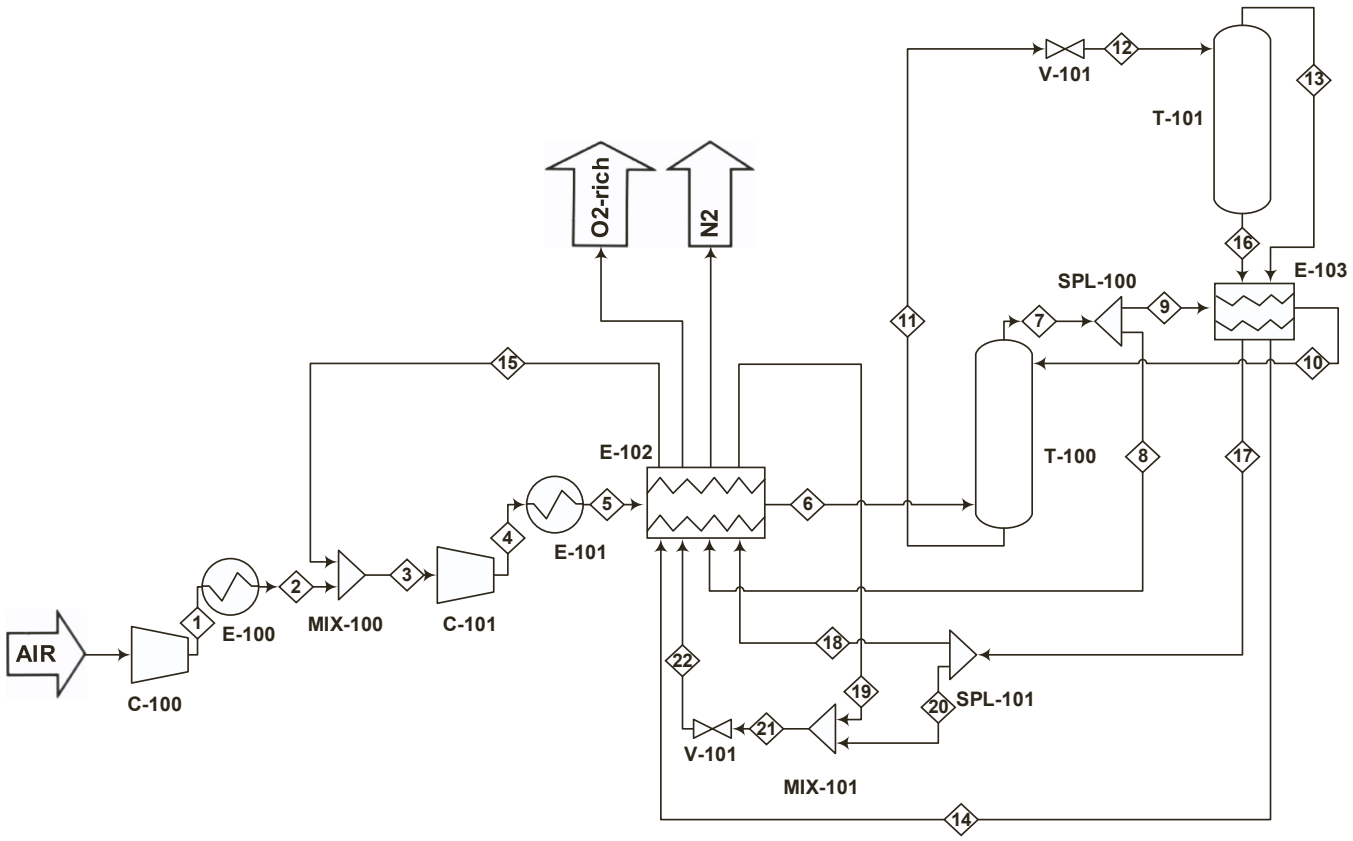

Fig. 4. N_2 separation process.

the separation is driven only toward the nitrogen. Several schemes are available in the literature to this purpose. In this work, the one proposed by Agrawal and Thorogood [42] is selected and simulated using Aspen Plus® V11 [27] to obtain material and energy balances useful for cost estimation following the procedure reported in Section 2.2.1. The RKS-BM (Redlich-Kwong-Soave Equation of State [43] with the alpha function modified as proposed by Boston and Mathias [44]), is selected as thermodynamic package.

Referring to the process illustrated in Fig. 4, the fed air stream undergoes compression to 8.5 bar in C-100 and C-101. An isentropic efficiency of 0.85 is assumed for the compressors. The minimum temperature approach inside the intercoolers E-100 and E-101 is 10 °C and they use CW as cold stream. The compressed air is then cooled to its dew point within heat exchanger E-102, which is characterized by a minimum temperature approach of 1 °C, since it operates at cryogenic temperatures. Subsequently, the cooled stream proceeds to the rectifying section of the distillation column (T-100). This column comprises 50 theoretical trays and operates at a high pressure of 8 bar. Its top product is in vapor phase and consists of pure N_2 (residual oxygen content of few ppm), and its bottom product consists of an approximately equimolar mixture of oxygen and nitrogen. This mixture is expanded to 3 bar and directed to the stripping section of the distillation column (T-101). At the top of this column, a stream resembling air's composition is obtained and it is then recycled back to the second compression stage C-101. Prior to this recycling, it passes through E-102 to cool the feed mixture. An oxygen-rich stream is obtained at the bottom of the same column and, after passing into E-102 as cold stream, leaves the system. The cooling duty required to condense part of the top product from T-100, which serves as the column's reflux, is obtained through the evaporation of the bottom product of the T-101. The power needed for the separation is all provided by compression. The resulting nitrogen stream serves as the feed for the subsequent ammonia synthesis stage.

Table 5
Streams conditions at the battery limits for the N_2 separation process (Fig. 4).

Stream		AIR	O2-rich	N2
T	[°C]	25	29.3	29.3
P	[bar]	1.01	3.05	8.04
molar fractions				
N_2		0.7900	0.4242	1.0000
O_2		0.2100	0.5758	0.0000
F_{TOT}	[kmol/h]	7,049.4	2,571.1	4,478.3

Table 6
Cooling duties of the N_2 separation process (Fig. 4).

Equipment	T_{IN} [°C]	T_{OUT} [°C]	Cooling duty [kW]
E-100	156.81	30	7,313.1
E-101	147.03	30	9,947.9

Table 7
Electric power consumptions of the N_2 separation process (Fig. 4).

Equipment	P_{IN} [bar]	P_{OUT} [bar]	Electric power [kW]
C-100	1.01	3.12	7,573.9
C-101	3.12	8.5	9,873.2

In Table 5 the inlet and outlet streams' conditions for the N_2 separation process are reported.

Table 6 and Table 7 report the energy balance for this process, detailing the cooling duties and electric power consumptions involved.

The Haber-Bosch NH_3 synthesis process is a well-established and widely applied large-scale industrial process. It is based on reaction (14) and its rate is enhanced by the presence of iron-based catalysts.

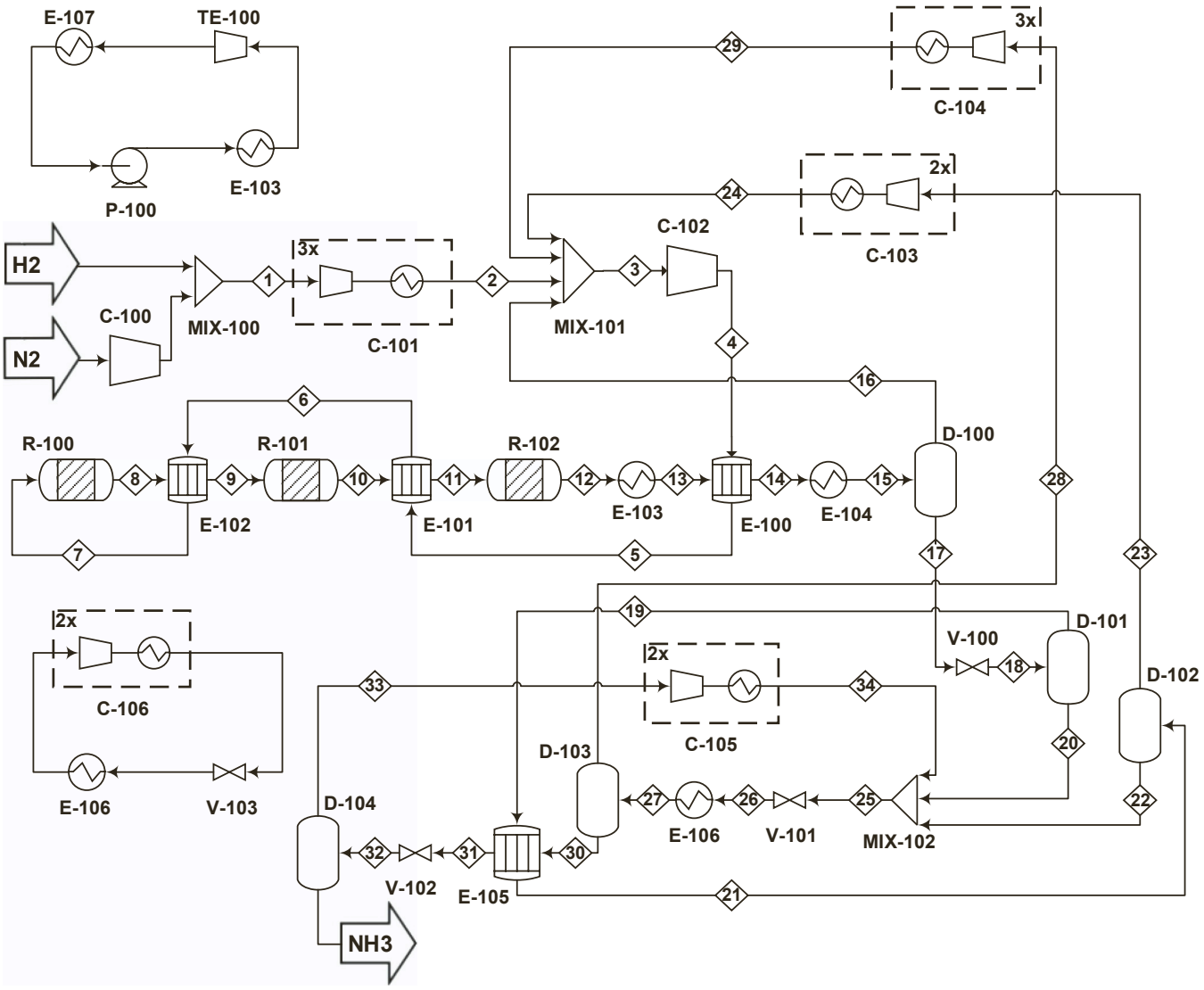

Fig. 5. NH_3 synthesis and liquefaction process [3].

$$3H_2 + N_2 \rightarrow 2NH_3 \quad (14)$$

For simulating the ammonia synthesis stage within Aspen Plus® V11 [27] and subsequently estimating its costs, reference is made to the work by Restelli et al. [3]. The RKS-BM thermodynamic package is selected for the simulation of this process. All the compressors and expanders are characterized by an isentropic efficiency of 0.85. The minimum temperature approach in the heat exchangers is 10 °C.

Referring to the ammonia synthesis process scheme, illustrated in Fig. 5, the nitrogen stream (N2), from the air separation process depicted in Fig. 4, is at 8 bar and 29 °C. It necessitates compression to 20 bar in C-100 before being mixed with the hydrogen stream (H2), sourced from RES-driven water electrolysis. The resulting mixture enters a three-stage compressor with intercooling (C-101). Downstream of the last post-cooler, it is at 30 °C and 193 bar and is mixed with the recycled streams, which are the vapors coming from the separators D-100, D-102 and D-103, after being compressed to 193 bar. Subsequently, this mixture is compressed to a pressure of 200 bar in C-102 and heated to a temperature of 347 °C through a series of three process-process heat exchangers (E-100, E-101 and E-102). These exchangers harness the high enthalpy content of products exiting the second and third stages of the reactor. The reaction section is composed of 3 adiabatic beds with intercooling. The Nielsen model [45] is implemented to describe the reaction kinetics. The sizing of the beds is optimized to minimize residence time for each stage, thus minimizing the required catalyst amount. After the reaction section, the produced NH_3 must be separated from the unreacted H_2 and N_2, which are then recycled, while also being cooled to the temperature needed for NH_3 liquefaction under nearly ambient pressure. The product purity must exceed 99.95 mol%. Downstream the reactor, the stream undergoes cooling in E-103 to 109 °C, providing heat to a steam Rankine cycle for electricity generation. Further cooling occurs downstream in E-104 using CW. The two-phase stream exiting E-104 is separated in flash drum D-100: the vapor is sent back to the reaction section, while the liquid undergoes further purification in a series of flash drums operating at decreasing pressures. Specifically, D-101 and D-102 operate at 30 bar, D-103 at 15 bar and D-104 at the storage pressure of 1.3 bar. The vapor from D-101 is cooled by exchanging heat in counter-current with the liquid from D-103 with the aim of condensing NH_3, which is then separated in D-102. This step helps avoid recycling a stream rich in the reaction product, which would shift the synthesis reaction (Eq. (14)) toward the left. The temperature of stream 27 at the outlet of E-106 is set to − 18 °C, and to achieve such a low temperature, a refrigeration cycle is employed with ammonia as refrigerant.

The inlet and outlet streams' conditions for the NH_3 synthesis and liquefaction process are reported in Table 8.

Table 9 and Table 10 report respectively the cooling duties and

Table 8
Streams conditions at the battery limits for the NH_3 synthesis and liquefaction process (Fig. 5).

Stream		H2	N2	NH3
T	[°C]	25	29.3	-29.0
P	[bar]	20	8.04	1.3
molar fractions				
H_2		1.0000	0.0000	0.0000
N_2		0.0000	1.0000	0.0000
NH_3		0.0000	0.0000	1.0000
F_{TOT}	[kmol/h]	13,435.0	4,478.3	8,956.7

Table 9
Cooling duties of the NH_3 synthesis and liquefaction process (Fig. 5).

Equipment	T_{IN} [°C]	T_{OUT} [°C]	Cooling duty [kW]
C-101 intercooler(1)	145.1	30	16,874.7
C-101 intercooler(2)	116.5	30	12,842.7
C-101 intercooler(3)	116.7	30	13,160.6
C-103 intercooler(1)	82.8	30	60.6
C-103 intercooler(2)	136.0	30	136.0
C-104 intercooler(1)	60.3	30	5.3
C-104 intercooler(2)	125.0	30	17.0
C-104 intercooler(3)	125.2	30	22.0
C-105 intercooler(1)	68.0	30	142.5
C-105 intercooler(2)	144.7	30	2,314.9
E-104	65.7	25	44,264.3
C-106 intercooler(1)	123.2	30	1,826.6
C-106 intercooler(2)	141.7	30	12,284.5
E-107	40.6	40.6	89,367.7

Table 10
Electric power consumptions of the NH_3 synthesis and liquefaction process (Fig. 5).

Equipment	P_{IN} [bar]	P_{OUT} [bar]	Electric power [kW]
C-100	8.04	20	3,852.0
C-101	20	193	40,011.2
C-102	193	200	1,553.8
C-103	30	193	226.5
C-104	15	193	46.9
C-105	1.3	15	737.6
C-106	1.5	16.32	3,953.4
P-100	0.06	20	97.4
TE-100	20	0.06	-34,387.9

electric power consumptions of such process.

Concerning the ammonia synthesis and liquefaction process (including the N_2 separation section), the economic assessment, performed in accordance with the methodology detailed in Section 2.2.1, results in *CAPEX* of 625.12 M€. A detailed breakdown of the bare module cost into the various equipment categories can be found in Table 11. By examining the pie chart within Table 11, it becomes evident that a substantial portion of the investment costs attributed to the ammonia synthesis process can be traced back to the reactor, heat exchangers and compressors.

It is assumed that 50 operators work in the ammonia synthesis plant. The *OPEX* are equal to 166.51 M€/y and their breakdown into *DMC*, *FMC* and *GE* is reported in Table 12. The utility costs are mainly due to the cost of the electric power consumed by compressors.

3.1.2. LNH_3 – maritime transport

The investment costs associated with the acquisition of the vessel and the operating costs associated with the crew labor, fuel consumption and related CO_2 emissions costs, maintenance and insurance are considered.

Assuming the purchase of a single ship, its gross capacity (V_{vessel}) is computed using Eq. (8) and results equal to 97,800 m^3. The cost for an 80,000 m^3 Liquefied Petroleum Gas (LPG) ship is available from the literature [46]. To adapt this cost for the desired capacity, a six-tenths rule is applied, resulting in *CAPEX* of 94.41 M€ for the present analysis.

The *OPEX* related to the crew labor, fuel consumption and CO_2 emissions are calculated according to Eqs. (9)-(11), considering a crew size of 31 people and a fuel consumption rate of 58.1 t/d, as indicated in the technical data sheet corresponding to a vessel of similar capacity to the one under study [47]. The total operating costs for the maritime transport of LNH_3 result 26.59 M€/y.

Throughout sea transport, the boil-off phenomenon leads to a loss of approximately 0.04% per day of ammonia [48,49]. It is assumed that this lost quantity is directed to a flare.

3.1.3. LNH_3 – storage

The liquefied ammonia is at approximately − 30 °C at nearly ambient pressure and it is stored inside tanks coated with polyurethane foam insulation to minimize losses due to boil-off. The investment costs associated with the acquisition of the storage tanks and the operating costs associated with maintenance and insurance are taken into consideration. Boil-off losses are deemed negligible given the possibility of recondensing the boil-off gas at the loading terminal and directing it to the partial cracking process at the unloading terminal.

Table 12
Breakdown of the OPEX [M€/y] for the ammonia synthesis and liquefaction process.

Cost item	Units	Value
DMC	[M€/y]	75.54
FMC	[M€/y]	48.80
GE	[M€/y]	42.17
OPEX	**[M€/y]**	**166.51**

Table 11
Breakdown of the CAPEX [M€] for the ammonia synthesis and liquefaction process.

Cost item	**Equipment**	Units	Value
C_{BM}	Heat Exchangers	[M€]	120.53
	Reactor	[M€]	207.58
	Compressors	[M€]	109.27
	Pumps	[M€]	0.11
	Turbines	[M€]	14.93
	Vessels	[M€]	12.42
	Columns	[M€]	4.76
C_{TM}		[M€]	554.13
CAPEX		**[M€]**	**625.12**

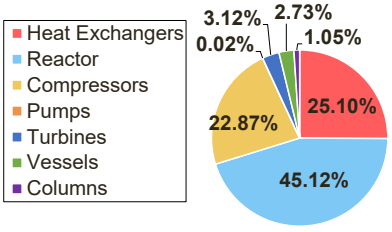

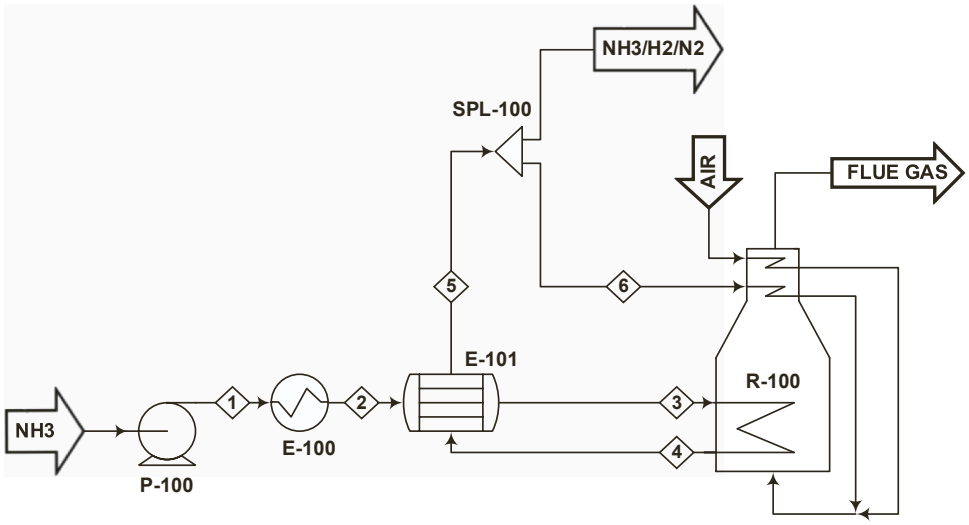

Fig. 6. Ammonia partial cracking process.

For each terminal, the required storage capacity ($V_{storage}$) is calculated using Eq. (13) and results equal to 107,500 m^3. It is considered to buy two storage tanks per terminal, having unit capacity of 55,000 m^3. The cost of a tank having a capacity of 44,300 m^3 is available from the literature [50]. This cost is inflation-adjusted to 2022 using the *CEPCI* and scaled for the capacity using the six-tenths rule. The total *CAPEX* and *OPEX* for the four storage tanks are 96.34 M€ and 9.63 M€/y, respectively.

3.1.4. LNH_3 – partial cracking

The decomposition of ammonia is an energetically demanding process because of the endothermicity of reaction (15). It typically occurs at high temperatures, which poses a significant challenge for its industrial-scale implementation.

$$2NH_3 \rightarrow 3H_2 + N_2 \quad (15)$$

The simulation of the partial cracking process is developed assuming the application of thermocatalytic technology, utilizing a nickel-based catalyst for ammonia decomposition into nitrogen and hydrogen.

The process is modeled using Aspen Plus® V11 [27] and its scheme is illustrated in Fig. 6. The RKS-BM thermodynamic package is selected for the simulation of this process.

Referring to the process scheme of Fig. 6, the fed liquid ammonia (NH3) undergoes pressurization to 10 bar in pump P-100, which is characterized by an isentropic efficiency of 0.8. It is subsequently preheated first in E-100 using CW, and then further in E-101 exploiting the high enthalpy of the reaction products. In the process-process heat exchanger E-101 the hot inlet - cold outlet temperature difference is 30 °C. This preheated stream is then directed to the cracking reactor (R-100), which is simulated using the RStoic module within Aspen Plus® V11 [27]. This approach is adopted due to the absence of comprehensive kinetic data in the current literature, making it challenging to build a reliable kinetic model. Thus, the heat requirement for the cracking reaction is calculated assigning the conversion of ammonia, equal to 30%, pressure and temperature of the reactor, equal to 10 bar and 500 °C, respectively. The necessary heat duty for the reactor is supplied by burning a portion of the product mixture, which in turn establishes the split ratio of SPL-100 between the product used as an internal utility within the process (stream 6) and the outgoing product (NH3/H2/N2). This approach eliminates the need for an external heat source. Air, slightly in excess of the stoichiometric amount to ensure complete combustion, is utilized as the oxidizer in the cracking furnace. The outgoing product mixture is then available for combustion in an ICE for power generation. An overview of the inlet and outlet streams' conditions for the partial cracking process is provided in Table 13.

Table 13
Streams conditions at the battery limits for the ammonia partial cracking process (Fig. 6).

Stream		NH3	FLUE GAS	AIR	NH3/H2/N2
T	[°C]	-27.6	140.5	25	35.1
P	[bar]	1.3	1.01	1.01	10
molar fractions					
NH_3		1.0000	0.0000	0.0000	0.5385
H_2		0.0000	0.0004	0.0000	0.3461
N_2		0.0000	0.7167	0.7900	0.1154
O_2		0.0000	0.0610	0.2100	0.0000
H_2O		0.0000	0.2167	0.0000	0.0000
NO		0.0000	0.0052	0.0000	0.0000
NO_2		0.0000	0.0000	0.0000	0.0000
N_2O		0.0000	0.0000	0.0000	0.0000
F_{TOT}	[kmol/h]	8,928.0	3,583.6	2,934.4	10,932.0

Table 14
Heating duty, provided by CW, and electric power consumption of the ammonia partial cracking process (Fig. 6).

Equipment	T_{IN} [°C]	T_{OUT} [°C]	Heating duty [kW]
E-100	-27.5	24.9	54,863.1
Equipment	P_{IN} [bar]	P_{OUT} [bar]	Electric power [kW]
P-100	1.3	10	68.0

Furthermore, the energy balance of the process, specifically concerning heating duty and electric power consumption, is detailed in Table 14.

Regarding the ammonia partial cracking, the *CAPEX* amount to 129.84 M€. The breakdown of the bare module cost across the different equipment categories is reported in Table 15. To determine the cost of the cracker, the equipment cost function of a pyrolysis furnace is used [37]. From the pie chart within Table 15, it is evident that almost all the capital expenses are due to the heat exchangers and reactor.

The *OPEX* of the ammonia partial cracking process are equal to 39.26 M€/y, and their breakdown into *DMC*, *FMC* and *GE* is reported in Table 16. The plant requires a workforce of 30 operators. Concerning utilities needed for the process, only the electric power necessary for pumping ammonia into the process is considered, and its cost is deemed negligible. Notably, no external fuel is required as the ammonia/hydrogen/nitrogen mixture is burned together with air to sustain the

Table 15
Breakdown of the *CAPEX* [M€] for the ammonia partial cracking process.

Cost item	Equipment	Units	Value
C_{BM}	Heat Exchangers	[M€]	51.24
	Reactor	[M€]	33.56
	Pump	[M€]	0.10
C_{TM}		[M€]	100.07
CAPEX		**[M€]**	**129.84**

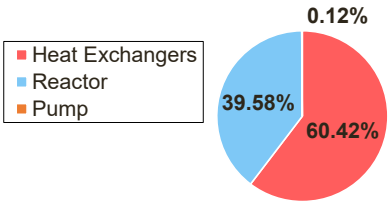

Table 16
Breakdown of the OPEX [M€/y] for the ammonia partial cracking process.

Cost item	Units	Value
DMC	[M€/y]	16.68
FMC	[M€/y]	12.30
GE	[M€/y]	10.28
OPEX	**[M€/y]**	**39.26**

endothermicity of the reaction (15). Throughout the economic assessment, the expenses related to NO_x emissions resulting from the combustion reaction are neglected, assuming to mitigate them through a non-catalytic ammonia-based process.

3.2. Fossil-based energy vector

Raw natural gas is extracted from gas or oil and gas reservoirs. The cost of natural gas production and processing depends on the characteristics of the reservoir (conventional/unconventional), location (onshore/offshore) and levels of impurities (CO_2, H_2S, mercaptans, …). A cost of 13 €/MWh is assumed for the natural gas, suitably purified to meet the LNG specifications, in the base case. According to the work by Zou et al. [51], this cost is in line with the upstream unit costs of LNG projects in the Middle East. A sensitivity analysis on the cost for production and purification of natural gas is performed to assess the impact of the assumed value on the results. The investigated range is 2 - 45 €/MWh. According to Ref. [51], values in the range 2 - 14 are realistic and reflective of the current scenario for natural gas production costs in the Middle East, while values as high as 45 €/MWh have been observed for certain projects in Norway and Australia. These high costs may be representative of cases involving the development of very sour reservoirs or reflect the market price during periods of shortage. The CO_2 emissions during production and processing are assumed to be 50 kg/MWh, which is an average value of the equivalent CO_2 (accounting for both hydrocarbons and CO_2 emissions) emitted during the pre-production (exploration, site preparation/construction and well completion), extraction and processing phases [52]. The costs for these emissions and for those during utilization are accounted using the SCC.

The LNG transport chain consists of liquefaction, maritime transport, storage and regasification. The techno-economic assessment of these blocks is detailed in the following sections.

3.2.1. LNG – liquefaction

The liquefaction of natural gas occurs at − 160 °C and atmospheric pressure. Several process schemes are commonly used in the industry to this purpose: propane precooled mixed refrigerant (C3MR) process [53–55], dual mixed refrigerant process [56–58], single mixed refrigerant process [59–61] and Phillips Cascade process [62,63] involving cooling with three pure refrigerant cycles. The most widespread process is certainly the C3MR cycle. It comprises a precooling cycle that uses propane as the refrigerant and a liquefaction cycle that uses a mixed refrigerant. The process, illustrated in Fig. 7, is simulated using Aspen Plus® V11 [27] to obtain material and energy balances, which are useful for cost estimation following the procedure outlined in Section 2.2.1. The GERG2008 [64] thermodynamic package is selected for this simulation due to its high accuracy in predicting the thermodynamic properties and phase equilibrium of natural gases and other mixtures consisting of natural gas components. All the compressors are characterized by an isentropic efficiency of 0.85. The minimum temperature approach in the multi-pass heat exchangers is 3 °C, while in the process-CW heat exchangers is 10 °C.

Referring to the process in Fig. 7, the natural gas stream (NG) coming from the dehydration and purification section is the inlet stream to the liquefaction process. The natural gas feed and the mixed refrigerant are pre-cooled in a series of four heat exchangers (E-100, E-101, E-102 and E-103). The precooling cycle consists of propane providing cooling at

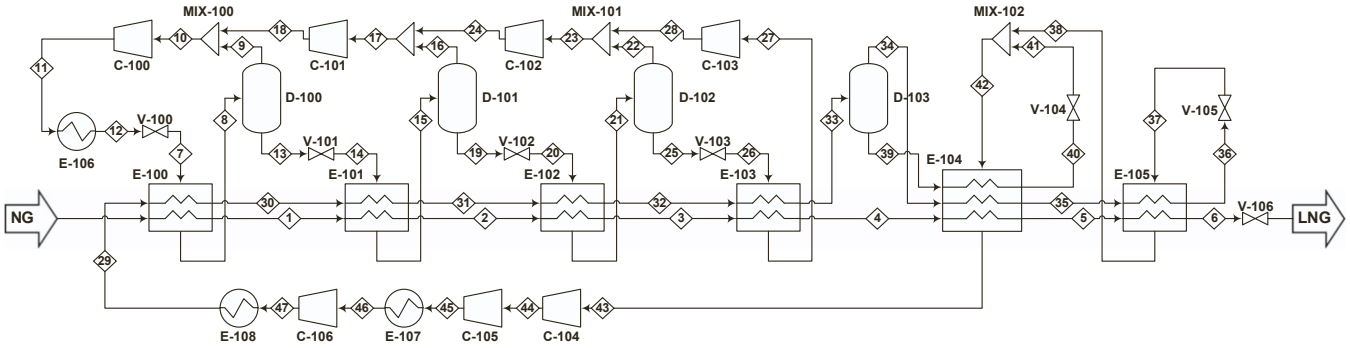

Fig. 7. Natural gas liquefaction process (C3MR process).

Table 17
Cooling duties of the natural gas liquefaction process (Fig. 7).

Equipment	T_{IN} [°C]	T_{OUT} [°C]	Cooling duty [kW]
E-106	45.4	30	172,532.65
E-107	57.2	30	19,573.37
E-108	104.0	30	64,484.15

Table 18
Electric power consumptions of the natural gas liquefaction process (Fig. 7).

Equipment	P_{IN} [bar]	P_{OUT} [bar]	Electric power [kW]
C-100	7.2	10.8	11,429.69
C-101	5.13	7.2	7,503.52
C-102	2.5	5.13	11,851.21
C-103	1.3	2.5	3,623.53
C-104	3.5	8.12	27,192.32
C-105	8.12	18.83	32,531.64
C-106	18.83	53	43,016.14

four evaporating pressures: 7.2 bar in E-100, 5.13 bar in E-101, 2.5 bar in E-102 and 1.3 bar in E-103. The propane refrigerant is compressed in four stages to reach a pressure of 10.8 bar, then is cooled using CW and sent to the train of throttling valves and separators to close the cycle. In the liquefaction cycle, a mixed refrigerant (consisting of 44 mol% methane, 41.72 mol% ethane, 8.48 mol% propane and 5.8 mol% nitrogen) is used to liquefy the natural gas in two multi-current heat exchangers (E-104 and E-105). The mixed refrigerant, which is partially condensed after precooling, is separated into its vapor and liquid phases. The liquid- and vapor-phase refrigerants and the natural gas are cooled in multi-current heat exchanger E-104. The refrigerant vapor (stream 35) is further cooled in a second exchanger E-105 and, upon pressure reduction to 3.5 bar, provides the final cooling to the natural gas. The liquid refrigerant (stream 40) is let down in pressure to 3.5 bar and mixed with the vapor refrigerant leaving E-105, providing cooling in E-104 as a single stream. The mixed refrigerant is compressed in three stages with intercooling using CW.

The energy balance of the natural gas liquefaction process is provided in Table 17 and Table 18, presenting cooling duties and electric power consumptions, respectively.

The economic assessment conducted on the natural gas liquefaction process results in *CAPEX* of 1,676.18 M€. The detailed breakdown of the bare module can be found in Table 19, from which it is possible to notice that the majority of investment costs are attributed to the heat exchangers and compressors.

It is assumed that a workforce of 200 operators is required for the plant's operation [65,66]. The OPEX, as detailed in Table 20, amount to 501.30 M€/y. Notably, a significant portion of utility costs is attributed to the electricity required for driving the compressors.

3.2.2. LNG – maritime transport

The investment costs associated with the acquisition of the ships and the operating costs associated with the labor, fuel and CO_2 emissions costs, maintenance and insurance are considered.

The gross capacity to be shipped is computed using Eq. (8) and results equal to 485,800 m^3. It is assumed to buy 3 ships, each with a gross capacity of 162,000 m^3, whose investment cost is obtained by interpolating with a power law of V_{vessel} the data available in the literature [67], and reported in Table 21, after being inflation-adjusted to the year 2022. The overall *CAPEX* result equal to 799.25 M€.

The operating costs related to the labor, fuel consumption and CO_2 emissions are calculated according to Eqs. (9)-(11) by considering a crew size of 27 people [68] and a fuel consumption of 5.4 t/d [69] for each ship. The total *OPEX* for the sea shipping of LNG results 181.45 M€/y.

During sea transport, approximately 0.13% of natural gas is lost daily due to the boil-off phenomenon [49,70]. While it's possible to utilize the boil-off gas for on-board heating or power generation, this analysis assumes that it is not recovered and is instead directed to a flare.

3.2.3. LNG – storage

The LNG is stored at approximately − 166 °C and nearly ambient pressure, inside tanks coated with perlite insulation to minimize losses caused by the boil-off phenomenon.

The investment costs associated with the acquisition of the storage tanks, along with the operating costs related to maintenance and insurance are considered. Boil-off losses are neglected given the possibility of reliquefying the boil-off gas at the loading terminal and sending it to the regasification process at the unloading terminal.

For each terminal, the capacity to be stored ($V_{storage}$) is calculated using Eq. (13) and results equal to 534,400 m^3. It is assumed to buy 4

Table 20
Breakdown of the OPEX [M€/y] for the natural gas liquefaction process.

Cost item	Units	Value
DMC	[M€/y]	235.50
FMC	[M€/y]	139.15
GE	[M€/y]	126.65
OPEX	**[M€/y]**	**501.30**

Table 21
Ship's gross capacity (V_{vessel} [m^3]), reference *CAPEX* [M$] and year, referring to the literature source [67].

V_{vessel} [m^3]	*CAPEX* [M$]	Year
135,000	170	2014
215,000	250	2014

Table 19
Breakdown of the CAPEX [M€] for the natural gas liquefaction process.

Cost item	Equipment	Units	Value
C_{BM}	Heat Exchangers	[M€]	787.42
	Compressors	[M€]	375.58
	Vessels	[M€]	12.85
	Coldboxes	[M€]	28.25
C_{TM}		[M€]	1,420.83
CAPEX		**[M€]**	**1,676.18**

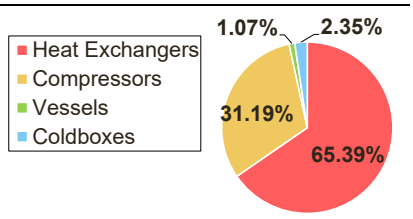

Table 22
Tank's gross capacity (V_{tank} [m^3]), reference *CAPEX* [M$] and year, referring to the literature source [71].

V_{tank} [m^3]	*CAPEX* [M$]	Year
28,388	60	2013
166,540	135	2013

tanks, having unit capacity of 134,000 m^3, per each terminal. The *CAPEX* for the LNG tank are taken from literature [71] and reported in Table 22. These costs are adjusted for inflation to 2022 using the *CEPCI* and interpolated with a power law to derive the *CAPEX* in function of the tank's gross volume.

The total *CAPEX* and *OPEX* result equal to 1,338.05 M€ and 133.81 M€/y, respectively.

3.2.4. LNG – regasification

The reconversion from liquid to gaseous natural gas consists in pumping and vaporization. The process diagram of the regasification process is depicted in Fig. 8. The simulation of the process is carried out using Aspen Plus® V11 [27] and selecting the GERG2008 as thermodynamic package.

The pump (P-100) discharge pressure is set to 30 bar. It is assumed a pump efficiency of 0.8 and CW as hot fluid in the vaporizer, consisting of economizer (E-100), evaporator (E-101) and superheater (E-102). The minimum approach temperature is achieved at the cold side outlet and is equal to 10 °C. The water is cooled to 20 °C, while warming the natural gas.

Table 23 presents the energy balance of the regasification process, outlining the heating duties and electric power consumption involved.

The regasification process involves *CAPEX* of 21.60 M€ (Table 24) and *OPEX* of 52.60 M€/y (Table 25). The plant requires a workforce of 60 operators.

3.3. Comparison between green and fossil-based energy vectors

The Block Flow Diagram (BFD) of the green and fossil-based energy vector value chains is reported in Fig. 9.

It is possible to observe that for the same amount of energy delivered, the moved mass is greater for the green energy vector since its energy content (heating value) is lower per unit mass with respect to LNG. For both the energy vectors, mass losses occur as boil-off during maritime transport. In addition, for the LNH_3, part of the fuel delivered is burned to sustain the endothermicity of the cracking reaction and, hence, considering also this loss, a greater amount of energy vector must be produced and transported.

The results in terms of *LCoE* for each block of the two investigated value chains are reported in Fig. 10 for the base case.

The cost for ammonia synthesis results higher than for natural gas liquefaction. This is due to the fact that the ammonia reactor operates at high pressure (200 bar) to enhance the kinetics of the synthesis reaction. On the other hand, refrigeration cycles used to liquefy natural gas has a maximum pressure lower than 20 bar. As regards the maritime transport cost, the *CAPEX* per unit volume for LNG vessels are higher than LNH_3 due to its thermophysical properties, which require a very low storage temperature with high-cost insulation materials, while the *OPEX* are lower because the capacity of LNG ship is lower due to its higher energy content (heating value). The environmental cost related to transport is due to the released methane as BOG and the fuel burned to power the ships.

The transportation cost of liquid ammonia is 5.61 €/MWh, while that of LNG is 4.69 €/MWh. The cost of transporting energy as LNH_3 is higher than LNG in terms of €/MWh because of the lower energy density of ammonia compared to LNG. On the other hand, the total transportation cost per unit mass is 0.030 €/kg and 0.065 €/kg for liquid ammonia and LNG, respectively. Ammonia has a lower cost per unit mass compared to LNG. Moreover, the total transport cost per unit volume is 20.50 €/m^3 and 30.63 €/m^3, respectively for LNH_3 and LNG. Therefore, for transporting substantial amounts of energy, liquefied ammonia proves to be more economically viable, considering the cost per cubic meter.

For the carbon-free energy vector, the overall *LCoE* is 231.71 €/MWh. Looking at Fig. 10, it is evident that the green hydrogen production has the highest impact on the overall cost of energy, followed by the ammonia synthesis process, while the cost for storage, transport and partial cracking does not influence the result significantly. The ammonia synthesis process is already well established due to its widespread use. However efforts are currently being made for a process intensification of the Haber-Bosch synthesis to try, by means of removal by absorption of the ammonia produced, to reduce the pressure level of the reaction [72,73]. The overall *LCoE* for the fossil-based energy vector is 59.19 €/MWh. From Fig. 10 it is possible to notice that the cost for the CO_2 emissions, related to the social cost of carbon, greatly influences the overall cost of energy, followed by the cost for natural gas production and processing and for liquefaction.

For the base case, in which a SCC of 0.100 €/kg is assumed, the traditional fossil-based energy carrier has a much lower cost with

Table 23
Heating duties, provided by CW, and electric power consumption of the LNG regasification process (Fig. 8).

Equipment	T_{IN} [°C]	T_{OUT} [°C]	Heating duty [kW]
E-100	-157.1	-95.9	34,368.3
E-101	-95.9	-95.9	37,127.1
E-102	-95.9	20	45,251.2
Equipment	**P_{IN} [bar]**	**P_{OUT} [bar]**	**Electric power [kW]**
P-100	1.3	30	1,180.3

Table 24
Breakdown of the CAPEX [M€] for the LNG regasification process.

Cost item	Equipment	Units	Value
C_{BM}	Heat Exchangers	[M€]	13.51
	Pumps	[M€]	0.83
C_{TM}		[M€]	16.93
CAPEX		**[M€]**	**21.60**

Table 25
Breakdown of the OPEX [M€/y] for the LNG regasification process.

Cost item	Units	Value
DMC	[M€/y]	18.47
FMC	[M€/y]	9.02
GE	[M€/y]	9.95
OPEX	**[M€/y]**	**37.44**

Fig. 8. LNG regasification process.

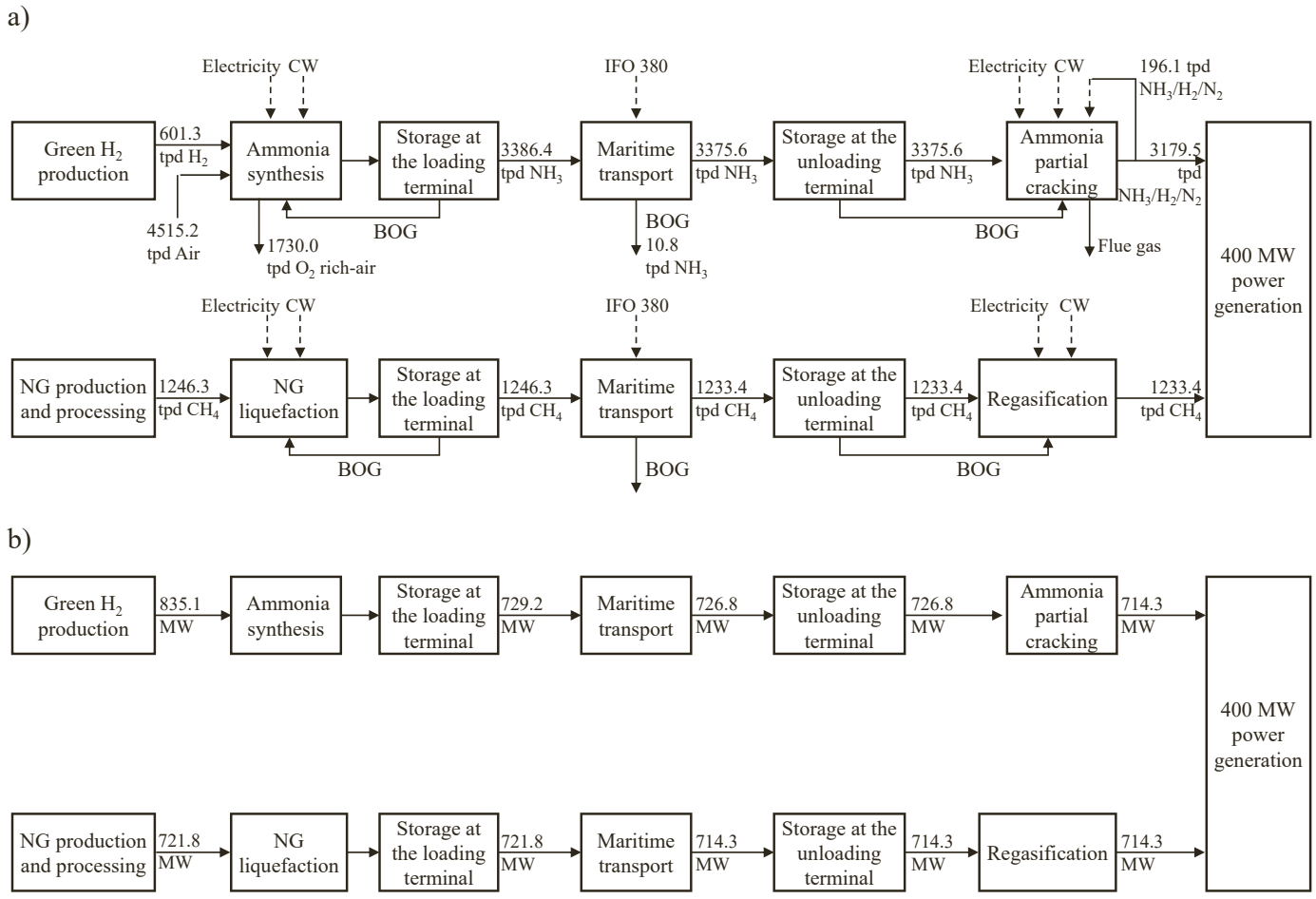

Fig. 9. BFD of the value chains of green and fossil-based energy vectors in terms of: a) mass and b) energy.

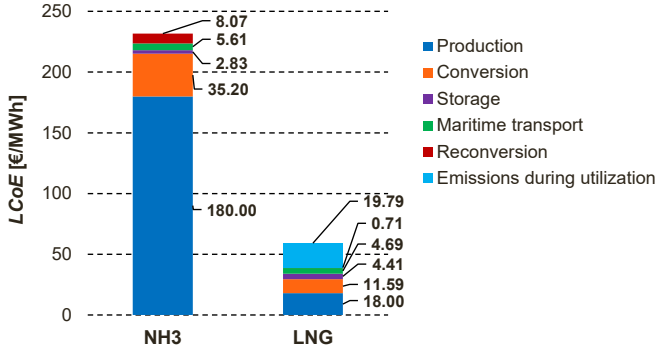

Fig. 10. *LCoE* [€/MWh] in the base case: comparison between the green and fossil-based energy vectors.

respect to the green energy vector. However, when the SCC is higher, ammonia can become competitive. In particular, for the base case, a break-even SCC of 0.797 €/kg is calculated.

The social cost of carbon required to break even the levelized cost of energy of the two value chains is computed as the production costs of green hydrogen and purified natural gas vary in the range of 60 - 400 €/MWh and 2 - 45 €/MWh, respectively, and the results are represented in Fig. 11.

As the SCC increases, the cost of emissions during utilization of natural gas increases dramatically. This increment favors liquid ammonia as an energy vector. In particular, when the production cost of green hydrogen is optimistically low (i.e. 60 €/MWh) and the cost of natural gas is high (i.e. 45 €/MWh) a SCC equal to 0.183 €/kg is required to break even the *LCoE* of the green and fossil-based energy vectors, as represented in Fig. 11d. For the sake of comparison, the average value of the EU ETS (European Emissions Trading System) in 2022 is 0.081 €/kg [74], about one half of the calculated SCC. On the other hand, when the most unfavorable scenario for the competitiveness of the green energy vector is considered (i.e. green hydrogen production cost as high as 400 €/MWh and purified natural gas cost as low as 2 €/MWh) a SCC of 1.731 €/kg is required for the break-even, as represented in Fig. 11a.

These results suggest that in the current scenario the adoption of ammonia (and of any other green energy vector) as a carbon-free energy vector is not economically advantageous. However, a combination of factors such as the cost of natural gas rising due to a period of shortage and a decrease in the cost of green hydrogen due to technological progress may occur in the future. This work provides a methodology to quantify the cost gap between the green ammonia and LNG value chains, which, if filled with an appropriate penalty that takes into account the negative impact of CO_2 emissions, makes the green energy vector economically, as well as environmentally, advantageous.

4. Conclusions

A comprehensive techno-economic evaluation of two value chains, namely ammonia as a green energy vector and LNG as a conventional fossil-based energy vector, has been performed. The aim of this work was to develop a methodology for comparing the value chains of two energy vectors, green ammonia and LNG, showing in quantitative terms what is the gap to be filled in order to make green processes feasible

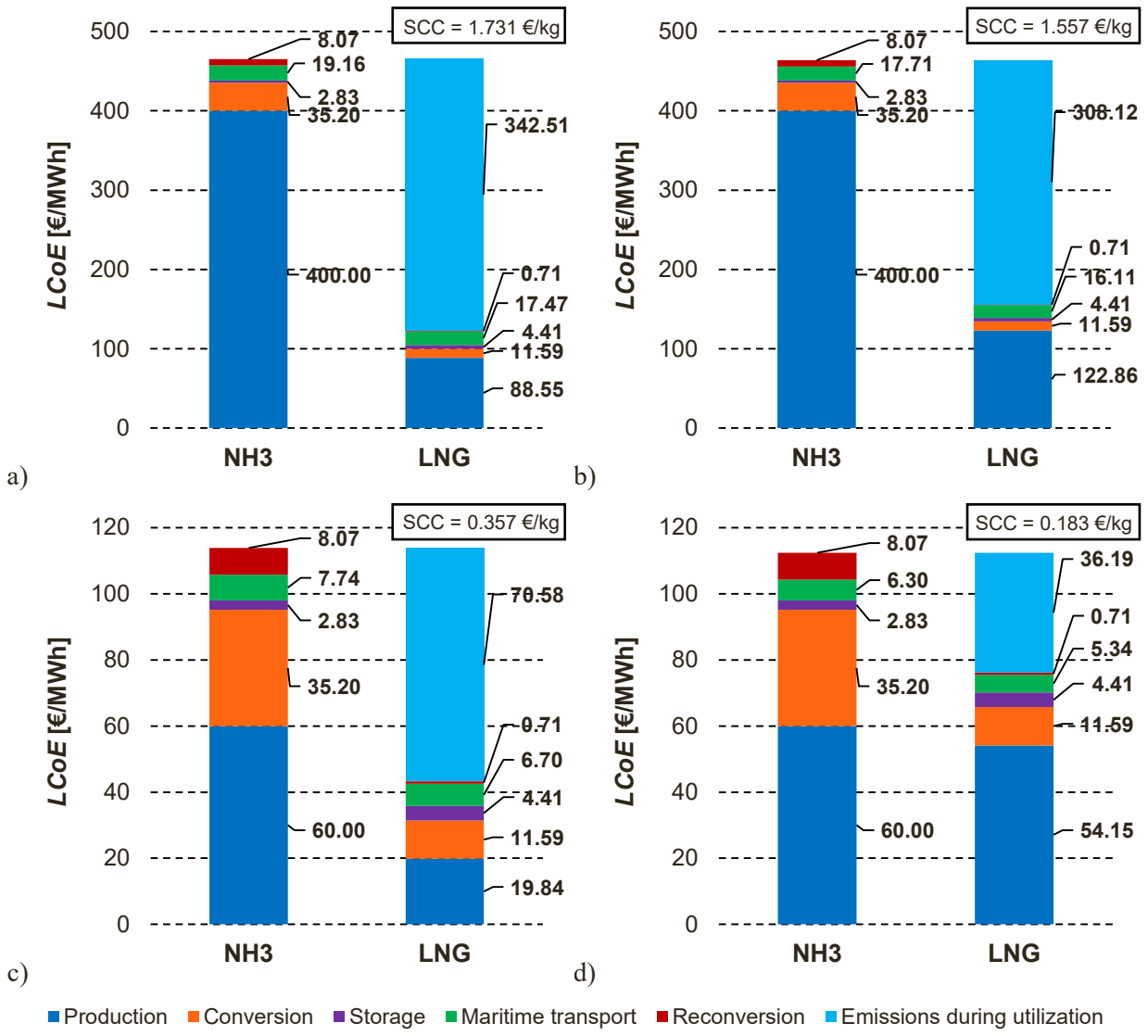

Fig. 11. *LCoE* [€/MWh] of the green and fossil-based energy vectors and break-even SCC [€/kg] for the cases of green hydrogen and purified natural gas production costs respectively of: a) 400 €/MWh and 2 €/MWh, b) 400 €/MWh and 45 €/MWh, c) 60 €/MWh and 2 €/MWh, d) 60 €/MWh and 45 €/MWh.

from an economic point of view.

The most cost-effective option, while considering the social cost of carbon, was pointed out, as well as the SCC required to favor the adoption of the green energy vector.

Considering a social cost of carbon of 0.100 €/kg, the *LCoE* of the LNG value chain is 59.19 €/MWh, while that of LNH_3 is 231.71 €/MWh. The overall cost of the LNG value chain, including natural gas production and processing, liquefaction, storage, transportation and utilization, is lower compared to the ammonia value chain, which involves green hydrogen production, ammonia synthesis and liquefaction, storage, transportation and partial cracking. This cost advantage stems from the well-established infrastructure and mature technologies associated with LNG, making it a highly efficient and cost-effective energy vector.

While the economic analysis favors LNG as the most cost-effective option at the current social cost of carbon, it is vital to consider other factors beyond the immediate financial aspects. Environmental considerations and the long-term sustainability of energy production are of paramount importance. Ammonia, being a green energy vector, offers significant potential for reducing carbon emissions and promoting a more sustainable energy future.

The social cost of carbon required to break even the levelized cost of energy of the two value chains has been calculated as the production costs of green hydrogen and purified natural gas vary. A SCC of 0.183 €/MWh is calculated in the most favorable scenario for the green energy vector, with a production cost of green hydrogen as low as 60 €/MWh and a cost of natural gas as high as 45 €/MWh. On the other hand, if the most unfavorable scenario is considered (i.e. green hydrogen production cost of 400 €/MWh and purified natural gas cost of 2 €/MWh) a break-even SCC of 1.731 €/kg is computed.

In conclusion, this techno-economic assessment highlights the cost-effectiveness of LNG as a conventional fossil-based energy vector in the current economic and regulatory landscape. However, the break-even range for the social cost of carbon indicates the potential for ammonia as a green energy vector to gain economic viability under higher carbon pricing scenarios. As the transition to a low-carbon economy progresses, further research and policy support are essential to unlock the full potential of green energy vectors like ammonia and ensure a sustainable energy future.

CRediT authorship contribution statement

Federica Restelli: Conceptualization, Methodology, Formal

analysis, Writing – original draft, Visualization. **Marta Gambardella:** Software, Investigation, Validation, Writing – original draft. **Laura Annamaria Pellegrini:** Conceptualization, Methodology, Writing – review & editing, Supervision.

Declaration of Competing Interest

The authors declare that they have no known competing financial interests or personal relationships that could have appeared to influence the work reported in this paper.

Data Availability

Data will be made available on request.

References

[1] M. Aziz, A.T. Wijayanta, A.B.D. Nandiyanto, Ammonia as effective hydrogen storage: a review on production, storage and utilization, Energies 13 (2020) 3062.
[2] A. Valera-Medina, H. Xiao, M. Owen-Jones, W.I.F. David, P.J. Bowen, Ammonia for power, Prog. Energy Combust. Sci. 69 (2018) 63–102.
[3] F. Restelli, E. Spatolisano, L.A. Pellegrini, A.R. de Angelis, S. Cattaneo, E. Roccaro, Detailed techno-economic assessment of ammonia as green H_2 carrier, Int. J. Hydrog. Energy 52 (2024) 532–547.
[4] F. Restelli, E. Spatolisano, L.A. Pellegrini, S. Cattaneo, A.R. de Angelis, A. Lainati, et al., Liquefied hydrogen value chain: a detailed techno-economic evaluation for its application in the industrial and mobility sectors, Int. J. Hydrog. Energy 52 (2024) 454–466.
[5] E. Spatolisano, F. Restelli, A. Matichecchia, L.A. Pellegrini, A.R. de Angelis, S. Cattaneo, et al., Assessing opportunities and weaknesses of green hydrogen transport via LOHC through a detailed techno-economic analysis, Int. J. Hydrog. Energy 52 (2024) 703–717.
[6] Y. Ishimoto, M. Voldsund, P. Nekså, S. Roussanaly, D. Berstad, S.O. Gardarsdottir, Large-scale production and transport of hydrogen from Norway to Europe and Japan: Value chain analysis and comparison of liquid hydrogen and ammonia as energy carriers, Int. J. Hydrog. Energy 45 (2020) 32865–32883.
[7] M. Raab, S. Maier, R.-U. Dietrich, Comparative techno-economic assessment of a large-scale hydrogen transport via liquid transport media, Int. J. Hydrog. Energy 46 (2021) 11956–11968.
[8] L. Kang, W. Pan, J. Zhang, W. Wang, C. Tang, A review on ammonia blends combustion for industrial applications, Fuel 332 (2023), 126150.
[9] Verkamp F.J., Hardin M.C., Williams J.R. Ammonia combustion properties and performance in gas-turbine burners. 1 ed: Elsevier. p. 985–992.
[10] https://dev.ammoniaenergy.org/articles/ammonia-fueled-solid-oxide-fuel-cell-advance-at-kyoto-university/. [Accessed 22 June 2023].
[11] IRENA and AEA. Innovation Outlook: Renewable Ammonia. 2022.
[12] https://www.mitsui.com/jp/en/topics/2023/1245792_13949.html. [Accessed 15 May 2023].
[13] The Royal Society. Ammonia: zero-carbon fertiliser, fuel and energy store. 2019.
[14] https://power.mhi.com/news/20210301.html. [Accessed 15 May 2021].
[15] https://www.ihi.co.jp/en/all_news/2020/resources_energy_environment/1197060_2032.html. [Accessed 15 May 2023].
[16] M. Tamura, T. Gotou, H. Ishii, D. Riechelmann, Experimental investigation of ammonia combustion in a bench scale 1.2 MW-thermal pulverised coal firing furnace, Appl. Energy 277 (2020), 115580.
[17] EPRI and L.C.R.I. Ammonia and hydrogen fuel blends for today's gas turbines: combustion consideration. 2021.
[18] IEA. The Future of Hydrogen. 2019.
[19] https://www.jogmec.go.jp/content/300381295.pdf. [Accessed 15 May 2023].
[20] S. Song, H. Lin, P. Sherman, X. Yang, C.P. Nielsen, X. Chen, et al., Production of hydrogen from offshore wind in China and cost-competitive supply to Japan, Nat. Commun. 12 (2021), 6953.
[21] A.T. Wijayanta, T. Oda, C.W. Purnomo, T. Kashiwagi, M. Aziz, Liquid hydrogen, methylcyclohexane, and ammonia as potential hydrogen storage: Comparison review, Int. J. Hydrog. Energy 44 (2019) 15026–15044.
[22] S. Giddey, S.P.S. Badwal, C. Munnings, M. Dolan, Ammonia as a renewable energy transportation media, ACS Sustain. Chem. Eng. 5 (2017) 10231–10239.
[23] N. Salmon, R. Banares-Alcántara, Green ammonia as a spatial energy vector: a review, Sustain. Energy Fuels 5 (2021) 2814–2839.
[24] J.S. Cardoso, V. Silva, R.C. Rocha, M.J. Hall, M. Costa, D. Eusébio, Ammonia as an energy vector: current and future prospects for low-carbon fuel applications in internal combustion engines, J. Clean. Prod. 296 (2021), 126562.
[25] R. Estevez, F.J. López-Tenllado, L. Aguado-Deblas, F.M. Bautista, A.A. Romero, D. Luna, Current research on green ammonia (nh3) as a potential vector energy for power storage and engine fuels: a review, Energies 16 (2023) 5451.
[26] A. Valera-Medina, F. Amer-Hatem, A.K. Azad, I.C. Dedoussi, M. De Joannon, R. X. Fernandes, et al., Review on ammonia as a potential fuel: from synthesis to economics, Energy Fuels 35 (2021) 6964–7029.
[27] AspenTech. Aspen Plus®,Burlington (MA), United States. 2019.
[28] IEA and NEA. Projected costs of generating electricity. 2020.
[29] https://www.repower.com/gruppo/news/centrale_teverola_2007. [Accessed 19 June 2023].
[30] O. Schmidt, A. Gambhir, I. Staffell, A. Hawkes, J. Nelson, S. Few, Future cost and performance of water electrolysis: An expert elicitation study, Int. J. Hydrog. Energy 42 (2017) 30470–30492.
[31] Pellegrini L.A., Langé S., De Guido G., Moioli S., Mikus O., Picutti B., et al. An innovative technology for natural gas sweetening by means of cryogenic distillation. p. 1–18.
[32] S. Mokhatab, W.A. Poe, J.Y. Mak, Handbook of natural gas transmission and processing: principles and practices, Gulf professional publishing,, 2018.
[33] https://www.ammoniaenergy.org/articles/saudi-arabia-to-export-renewable-energy-using-green-ammonia/. [Accessed 22 June 2023].
[34] Lorenczik S., Kim S., Wanner B., Bermudez Menendez J.M., Remme U., Hasegawa T., et al. Projected costs of generating electricity-2020 edition. 2020.
[35] https://www.ecb.europa.eu/stats/policy_and_exchange_rates/euro_reference_exchange_rates/html/eurofxref-graph-usd.en.html. [Accessed 24 March 2023].
[36] https://www.statista.com/statistics/1322214/carbon-prices-european-union-emission-trading-scheme/. [Accessed 27 October 2023].
[37] R. Turton, R.C. Bailie, W.B. Whiting, J.A. Shaeiwitz, Analysis, synthesis and design of chemical processes, Pearson Education,, 2008.
[38] K.M. Guthrie, Capital Cost Estimating, Chem. Eng. 76 (1969) 114.
[39] Rogers H. LNG Shipping Forecast: costs rebounding, outlook uncertain. 2018.
[40] https://www.eia.gov/environment/emissions/co2_vol_mass.php. [Accessed 24 March 2023].
[41] Strategy E. Hydrogen Innovation Report 2022. 2022.
[42] R. Agrawal, R.M. Thorogood, Production of medium pressure nitrogen by cryogenic air separation, Gas. Sep. Purif. 5 (1991) 203–209.
[43] G. Soave, Equilibrium constants from a modified Redlich-Kwong equation of state, Chem. Eng. Sci. 27 (1972) 1197–1203.
[44] Boston J.F., Mathias P.M. Phase equilibria in a third-generation process simulator. Deutsche Gesellschaft für Chemisches Apparatewesen Great Neck, NY. p. 823–849.
[45] A. Nielsen, J. Kjaer, B. Hansen, Rate equation and mechanism of ammonia synthesis at industrial conditions, J. Catal. 3 (1964) 68–79.
[46] https://capitallinkshipping.com/wp-content/uploads/2022/10/Intermodal-Report-Week-41–2022_compressed.pdf. [Accessed 24 March 2023].
[47] https://www.icedesign.info/wp-content/uploads/ICE-84000-cu-m-LPG-Carrier-Design-2018.pdf. [Accessed 20 June 2023].
[48] P. Baboo, Ammonia Storage Tank Pre -Commissioning, Int. J. Eng. Res. Technol. 8 (2019) 612–624.
[49] J. Kim, C. Huh, Y. Seo, End-to-end value chain analysis of isolated renewable energy using hydrogen and ammonia energy carrier, Energy Convers. Manag. 254 (2022), 115247.
[50] Leighty W.C., Holbrook J.H. Alternatives to electricity for transmission and low-cost firming storage of large-scale stranded renewable energy as pipelined hydrogen and ammonia carbon-free fuels.
[51] Zou Q., Yi C., Wang K., Yin X., Zhang Y. Global LNG market: supply-demand and economic analysis. 1 ed: IOP Publishing. p. 012051.
[52] P. Balcombe, K. Anderson, J. Speirs, N. Brandon, A. Hawkes, Methane and CO_2 emissions from the natural gas supply chain: an evidence assessment: Sustainable Gas Institute, Imperial College London London,, 2015.
[53] L. Gaumer, C. Newton, Combined cascade and multicomponent refrigeration system and method, Google Pat. (1973).
[54] A. Alabdulkarem, A. Mortazavi, Y. Hwang, R. Radermacher, P. Rogers, Optimization of propane pre-cooled mixed refrigerant LNG plant, Appl. Therm. Eng. 31 (2011) 1091–1098.
[55] A. Mortazavi, C. Somers, Y. Hwang, R. Radermacher, P. Rodgers, S. Al-Hashimi, Performance enhancement of propane pre-cooled mixed refrigerant LNG plant, Appl. Energy 93 (2012) 125–131.
[56] H.F. Grootjans, R.K. Nagelvoort, K.J. Vink, Liquefying a stream enriched in methane, Google Pat. (2002).
[57] J.-H. Hwang, M.-I. Roh, K.-Y. Lee, Determination of the optimal operating conditions of the dual mixed refrigerant cycle for the LNG FPSO topside liquefaction process, Comput. Chem. Eng. 49 (2013) 25–36.
[58] I. Lee, I. Moon, Economic optimization of dual mixed refrigerant liquefied natural gas plant considering natural gas extraction rate, Ind. Eng. Chem. Res. 56 (2017) 2804–2814.
[59] Swenson L.K. Single mixed refrigerant, closed loop process for liquefying natural gas. 1977.
[60] A. Rehman, M.A. Qyyum, K. Qadeer, F. Zakir, X. He, A. Nawaz, et al., Single mixed refrigerant LNG process: Investigation of improvement potential, operational optimization, and real potential for further improvements, J. Clean. Prod. 284 (2021), 125379.
[61] M.A. Qyyum, N.V.D. Long, L.Q. Minh, M. Lee, Design optimization of single mixed refrigerant LNG process using a hybrid modified coordinate descent algorithm, Cryogenics 89 (2018) 131–140.
[62] C.G. Houser, J. Yao, D.L. Andress, W.R. Low, Efficiency improvement of open-cycle cascaded refrigeration process, Google Pat. (1997).
[63] M.F.M. Fahmy, H.I. Nabih, M. El-Nigeily, Enhancement of the efficiency of the open cycle phillips optimized cascade LNG process, Energy Convers. Manag. 112 (2016) 308–318.
[64] O. Kunz, W. Wagner, The GERG-2008 wide-range equation of state for natural gases and other mixtures: an expansion of GERG-2004, J. Chem. Eng. data 57 (2012) 3032–3091.
[65] https://careersinenergy.ca/plan-your-future/working-in-lng/. [Accessed 27 October 2023].
[66] Songhurst B. LNG plant cost escalation. 2014.

[67] Fikri M., Hendrarsakti J., Sambodho K., Felayati F., Octaviani N., Giranza M., et al. Estimating capital cost of small scale LNG carrier. p. 5–6.
[68] http://www.poten.com/wp-content/uploads/2015/05/Tanker_Opinion_20070215.pdf. [Accessed 22 June 2023].
[69] https://www.man-es.com/docs/default-source/marine/tools/propulsion-trends-in-container-vessels.pdf?sfvrsn=c48bba16_12. [Accessed 22 June 2023].
[70] P. Głomski, R. Michalski, Problems with determination of evaporation rate and properties of boil-off gas on board LNG carriers, J. Pol. CIMAC 6 (2011) 133–140.
[71] https://www.interiorgas.com/wpdm-package/lng-storage-tank-cost-analysis/. [Accessed 23 June 2023].
[72] E. Spatolisano, L.A. Pellegrini, Haber-Bosch process intensification: a first step towards small-scale distributed ammonia production, Chem. Eng. Res. Des. (2023).
[73] C. Smith, A.K. Hill, L. Torrente-Murciano, Current and future role of Haber–Bosch ammonia in a carbon-free energy landscape, Energy Environ. Sci. 13 (2020) 331–344.
[74] https://icapcarbonaction.com/en/ets/eu-emissions-trading-system-eu-ets. [Accessed 26 June 2023].